Magnetic Ordering in Dilute Solid Solutions of Iron in Gold. I*

C. E. VIOLET AND R. J. BORG
Lawrence Radiation Laboratory, University of California, Livermore, California
(Received 15 April 1966)

Magnetic ordering in Au-Fe solid solutions with Fe concentrations between 0.8 and 8.0 at.% has been studied using the Mössbauer effect. The relative internal field for all solute concentrations scales with the reduced temperature and agrees qualitatively with either the α-Fe magnetization curve or a Brillouin curve with $S=1$. The value of the hyperfine field extrapolated to zero Fe concentration and 0°K is $(66\pm3)\%$ of its value in α Fe. The resonance lines in the magnetic hyperfine spectra are broader than the paramagnetic-resonance lines, possibly because of an intrinsic width of the hyperfine field ($\approx10\%$), or relaxation effects. The magnetic transition temperature varies approximately as the square root of the Fe concentration. A positive quadrupole coupling is observed for Fe concentrations of 6.7 and 7.4 at.%, but is not detectable in the more dilute alloys. The isomer shift is essentially independent of Fe concentration. Temperature hysteresis is observed near the ordering temperature for an Fe concentration of 6.7 at.%, but it is not detectable for an Fe concentration of 1.7 at.%.

I. INTRODUCTION

MEASUREMENT of the magnetic properties of solid solutions composed of diamagnetic solvents and paramagnetic solutes is a powerful method of investigating the interactions between magnetic atoms in metals.[1–16] Zener[1] proposed that an exchange interaction between the spins of the paramagnetic solute atom and the conduction electron might provide a mechanism for magnetic ordering in some metals and suggested this phenomenon be investigated in the Cu-Mn system. This prompted extensive investigations of the Cu-Mn system,[17–21] but until recently other alloy systems have remained largely unexplored. Accordingly, almost all theoretical work on dilute alloy magnetism has been directed toward a description of the Cu-Mn system.[4,6,13,14,21]

The study of the magnetic properties of the Au-Fe system using the Mössbauer effect is particularly advantageous because of (1) the relatively high solubility of Fe in Au which allows one to retain by quenching the primary solid solution containing up to about 30 at.% Fe concentration; (2) the relatively large magnetic moment of Fe; and (3) the readily observable Mössbauer transition of Fe^{57}.

The magnetic properties of the Au-Fe system were studied by conventional methods[22–27] before the Mössbauer investigations of Borg, Booth, and Violet[28] (henceforth abbreviated BBV). Kaufmann *et al.*[25] concluded that Au-Fe alloys containing less than about 6.5 at.% Fe were paramagnetic at all temperatures, whereas the more concentrated alloys appeared to possess definite Curie temperatures. Subsequently, several theoretical attempts were made to estimate the critical solute concentration below which ferromagnetic ordering would be unobtainable. The estimates[6,10,12] range between $(z-1)^{-1}\lesssim x\lesssim 2z^{-1}$ where x is the atomic fraction of solute atoms and z is the number of nearest neighbors. For the fcc lattice symmetry of Au-Fe alloys, $z=12$ and a critical concentration between 9–17 at.% would be expected. Arrott[29] calculated from the measurements of Kaufmann *et al.*[25] a value of 12 at.% for the critical Fe concentration in Au-Fe which Sato *et al.*[6] concluded to be in reasonable agreement with their theoretical value of 17 at.%.

Using the Mössbauer effect, BBV demonstrated that magnetic order is present at low temperatures in Au-Fe alloys with Fe concentrations as low as $x=0.84$ at.%. To account for these results it is necessary to assume some mechanism of indirect exchange. This discovery has since been confirmed by other investigators using

* Work performed under the auspices of the U. S. Atomic Energy Commission.

[1] C. Zener, Phys. Rev. **87**, 440 (1951).
[2] M. A. Ruderman and C. Kittel, Phys. Rev. **96**, 99 (1954).
[3] T. Kasuya, Progr. Theoret. Phys. (Kyoto) **16**, 45 (1956).
[4] K. Yosida, Phys. Rev. **106**, 893 (1957).
[5] A. Blandin and J. Friedel, J. Phys. Radium **20**, 160 (1959).
[6] H. Sato, A. Arrott, and R. Kikuchi, J. Phys. Chem. Solids **10**, 19 (1959).
[7] R. Brout, Phys. Rev. **115**, 824 (1959).
[8] A. W. Overhauser, J. Phys. Chem. Solids **13**, 71 (1960).
[9] A. W. Overhauser, Phys. Rev. Letters **3**, 414 (1959).
[10] J. S. Smart, J. Phys. Chem. Solids **16**, 169 (1960).
[11] A. W. Overhauser, J. Appl. Phys. **34**, 1019 (1963).
[12] S. H. Charap, Phys. Rev. **126**, 1393 (1962).
[13] M. W. Klein and R. Brout, Phys. Rev. **132**, 2412 (1963).
[14] M. W. Klein, Phys. Rev. **136**, A1156 (1964).
[15] J. Friedel, Can. J. Phys. **34**, 1190 (1956).
[16] J. Crangle and W. R. Scott, J. Appl. Phys. **36**, 921 (1965).
[17] J. Owen, M. Browne, W. D. Knight, and C. Kittel, Phys. Rev. **102**, 1501 (1956).
[18] J. Owen, M. Browne, V. Arp, and A. F. Kip, J. Phys. Chem. Solids **2**, 85 (1957).
[19] I. S. Jacobs and R. W. Schmidt, Phys. Rev. **113**, 459 (1959).
[20] R. W. Schmidt and I. S. Jacobs, J. Phys. Chem. Solids **3**, 324 (1957).
[21] J. S. Kouvel, J. Phys. Chem. Solids **24**, 795 (1963).
[22] J. W. Smith, Phys. Rev. **38**, 2051 (1931).
[23] E. R. Jette, W. L. Bruner and F. Foote, Trans. AIME **111**, 354 (1934).
[24] S. T. Pan, A. R. Kaufmann, and F. Bitter, J. Chem. Phys. **10**, 318 (1942).
[25] A. R. Kaufmann, S. T. Pan, and J. R. Clark, Rev. Mod. Phys. **17**, 87 (1945).
[26] E. Kronquist, Arkiv Fysik **5**, 453 (1952).
[27] E. Scheil, H. Specht, and E. Wachtel, Z. Metallk. **49**, 590 (1958).
[28] R. J. Borg, R. Booth, and C. E. Violet, Phys. Rev. Letters **11**, 464 (1963).
[29] A. Arrott, Phys. Rev. **108**, 1394 (1957).

bulk-magnetization measurements,[30–32] as well as the Mössbauer effect.[33,34] The presence of low-temperature transitions presumably magnetic in origin has also been inferred from electrical-resistivity measurements of Au-Fe alloys.[35–37]

In the bulk-magnetization measurements of Crangle and Scott[38] no finite Curie temperature could be measured in Au-Fe alloys with Fe concentration of 11 at.% or less. Consequently, these authors objected to the conclusion of BBV and set forth a model which assumes most of the Fe in the alloy is located within Fe-rich clusters. These regions are assumed to be superparamagnetic and independent of each other. In this model the transition temperatures in the dilute alloys would then correspond to the intrinsic Curie temperatures associated with the Fe-rich regions.

BBV and Henry[30] concluded from their data that the ordering is neither simple ferromagnetic or antiferromagnetic. However, Arrott[39] concluded that these data were completely consistent with antiferromagnetic ordering. Craig and Steyert[33] observed the Mössbauer resonance spectrum from a 5 at.% Fe alloy at 4.2°K in an applied magnetic field of 30.8 kOe. The absence of any detectable magnetization implies that the magnetic order averged over this sample is predominantly antiferromagnetic. Their experiment does not specify the intimate nature of the ordering nor does it preclude the possibility that perhaps 5% of the Fe spins are aligned ferromagnetically.

The Mössbauer effect provides a powerful method of measuring the magnetic field at the nucleus, as well as the critical temperature for magnetic ordering. As in other types of spectroscopy this method permits one to examine the average properties of single atoms, rather than of assemblages of atoms. Thus, the Mössbauer effect is an important adjunct to the more conventional experimental methods.

The hyperfine field (i.e. the magnetic field at the nucleus) is proportional to the time average of the z component of the Fe atom spin.[40] Thus, if the spin correlation time is short compared to the Zeeman transition periods, the positions of the resonance lines in the magnetic hyperfine spectrum will be proportional to the magnetization.[41,42]

For Fe concentrations less than 8–10 at.% the magnetic hyperfine spectrum exhibits (1) symmetric resonance lines with no detectable structure, and (2) line intensities which are in the ratios 3:2:1:1:2:3. The magnetic hyperfine spectra for Fe concentrations greater than 8–10 at.% exhibit neither of these properties.[43] Measurements on the dilute region will be presented in two parts; this paper being the first part. Paper II is currently being prepared for publication.

II. EXPERIMENTAL

The Mössbauer spectrometer is of the constant-velocity type and has been described in detail elsewhere.[44]

A cryostat is used to maintain sample temperatures between ≈ 2°K and room temperature. Sample temperatures can be varied by the use of an appropriate coolant, e.g., liquid He, H_2, and N_2, and a resistance heater. The sample temperature is measured using a carbon resistor which is also one leg of a resistance bridge. The temperatures are determined from the measured resistance and the following function[45]:

$$\ln R + K/\ln R = A + BT,$$

which is established experimentally. To prevent the occurrence of significant temperature gradients across the sample, both faces of the sample are covered with 25-μ-thick Al foil. The accuracy of the temperature measurements between 2.4°K and 30°K is ± 0.2°K. The sensitivity of the temperature adjustment is better than ± 0.1°K.

III. SAMPLE PREPARATION

With but one exception, alloy specimens were studied as absorbers rather than sources because of the greater ease of heat treating the former. Since the mean free path for 14.4 keV gamma rays in Au is ≈ 5 mg/cm^2, or $\approx 2.5\,\mu$, extremely thin absorbers must be prepared. They were originally made by vacuum evaporation. In this procedure[46] an Au film is first deposited on a Ni substrate coated with NaCl. The film is then removed by flotation. A specified amoung of Fe enriched with Fe^{57} ($Fe^{57}/Fe = 92\%$)[47] is then deposited on the free Au film. The composite film is then annealed *in situ* for 2 h at 850°C. All samples were made under the same source-substrate geometry. The pressure during deposition is approximately 10^{-6}–10^{-7} Torr. The foil is then quenched by flooding the furnace with argon.

Because the efficiency [(Fe deposited on the foil)/

[30] W. E. Henry, Phys. Rev. Letters **11**, 468 (1963).
[31] O. S. Lutes and J. L. Schmidt, Phys. Rev. **134**, A676 (1964).
[32] W. E. Henry, Bull. Am. Phys. Soc. **10**, 1101 (1965).
[33] P. R. Craig and W. A. Steyert, Phys. Rev. Letters **13**, 802 (1964).
[34] U. Gonser, R. W. Grant, C. J. Meecham, A. H. Muir, and H. Wiedersich, J. Appl. Phys. **36**, 2124 (1965).
[35] A. N. Gerritsen and J. O. Linde, Physica **17**, 573 (1951).
[36] A. N. Gerritsen, Physica **23**, 1087 (1957).
[37] R. C. Sundahl, T. Chen, J. M. Sivertsen, and Y. Sato, J. Appl. Phys. Suppl. **37**, 1024 (1966).
[38] J. Crangle and W. R. Scott, Phys. Rev. Letters **12**, 126 (1964).
[39] A. Arrott, Bull. Am. Phys. Soc. **9**, 114 (1964).
[40] A. J. Freeman, Phys. Rev. **130**, 888 (1963).
[41] F. van der Woude and A. J. Dekker, Phys. Status Solidi **9**, 775 (1965).
[42] M. Blume, Phys. Rev. Letters **14**, 96 (1965).
[43] C. E. Violet, Bull. Am. Phys. Soc. **9**, 499 (1964).
[44] R. Booth and C. E. Violet, Nucl. Instr. Methods **25**, 1 (1963).
[45] J. R. Clement and E. H. Quinnel, Rev. Sci. Instr. **23**, 213 (1952).
[46] W. F. Brunner and H. G. Patton, *1961 Transactions The Eighth National Vacuum Symposium—Second International Congress on Vacuum Science and Technology* (Pergamon Press, Inc., New York, 1962), Vol. II, p. 895.
[47] Obtained from Oak Ridge National Laboratory.

TABLE I. Characteristics of resonance lines at 77°K.

Sample	Fe concentration (at.%)	A (%)[a]	t[b]	Γ_0(calc) (mm/sec)	Γ_0(obs)[c] (mm/sec)	Γ_3[d]	Γ_2[d]	Γ_1[d]
AuFe-7	6.7	36	2.2	0.30	0.28±0.03	0.93	0.65	0.50
AuFe-9	1.7	14	0.53	0.25	0.31±0.03	0.83	0.55	0.40

[a] The total resonance absorption corrected for background.
[b] The effective absorber thickness (dimensionless).
[c] Resolved paramagnetic lines in class-III spectra.
[d] Full width at half-maximum (mm/sec). The rms error is ±0.03 mm/sec.

(Fe evaporated)] is low in this method, samples were subsequently prepared by melting milligram amounts of Fe^{57} and Au under high vacuum. The resulting buttons were rolled, diced, and remelted several times to insure homogeneity before finally being rolled into foils. It was found necessary to anneal foils prepared by either method an additional 8 to 16 h at 850°C. After this "homogenization anneal" no further change in the Mössbauer spectrum occurred with subsequent heat treatments. The homogenization anneal was terminated by quenching the quartz ampule containing the foil in water. All samples except AuFe-11 included in this paper were prepared by vacuum evaporation. The Fe concentrations of the samples were determined to an accuracy of ±10% by chemical analysis.

A deliberate attempt was made to induce precipitation of Fe by cold-working a foil containing 7.4 at.% Fe (AuFe-1) and then annealing the foil at several temperatures ranging from 100 to 210°C for several days. No change in the Mössbauer resonance spectrum was observed following such treatments, and we conclude that all Au-Fe alloys included in this paper consisted of single-phase solid solutions. Fe has been deliberately precipitated from more concentrated alloys, and the spectrum of α-Fe is readily distinguishable from the solid-solution spectrum.

To check the possibility that the Au matrix is itself polarized at low temperature,[39] a Co^{57} source (S-5) was prepared on a pure Au foil. Ten mCi of Co^{57} was electroplated on a 25-μ Au foil and then annealed *in vacuo* at 900°C for 12 h. This source was studied in conjunction with a 25-μ 310 stainless-steel absorber.

IV. SOURCES

A palladium source[48] was used to obtain most of the data; however, data previously reported[28] and included in this paper were obtained with a 310 stainless-steel (SS) source. The characteristics of both were studied using sodium ferrocyanide absorbers. Significantly narrower linewidths (and somewhat smaller Mössbauer effect) were obtained with the Pd source. Extrapolating to zero absorber thickness, gives for the full width at half-maximum

$$\Gamma_N(\text{Pd source}) = 0.23 \pm 0.01 \text{ mm/sec},$$

and

$$\Gamma_N(\text{SS source}) = 0.40 \pm 0.01 \text{ mm/sec}.$$

In the absence of experimental broadening the expected value of Γ_N is 0.194±0.002 mm/sec, based on the measured lifetime of the Fe^{57} 14-keV transition.[49] Since instrumental broadening is too small to account for the increased observed linewidth,[44] it presumably results from crystalline-field effects in the sources or absorbers.

In Table I the observed width Γ_0 of resolved paramagnetic lines of AuFe-7 and AuFe-9 with the Pd source are compared with widths calculated from the following equation[50]: $\Gamma_0 = \Gamma_N(1+0.135t)$ where

$$\Gamma_N = 0.23 \text{ mm/sec}$$

and t is the effective absorber thickness. Values of t in Table I are obtained from the maximum resonance absorption[50] using for the recoiless fraction of the Pd source, $f_s = 0.65$.[51] The agreement between observed and calculated linewidths is satisfactory.

V. ANALYSIS OF SPECTRA

A. Classification of Spectra

A representative series of spectra from two alloys, AuFe-7 and AuFe-9, showing the effect of Fe concentration and temperature, are shown in Figs. 1 and 2. Based on their appearance the spectra may be put into three classes, each requiring a different method for the extraction of information. These classes are: (I) magnetic hyperfine spectra for which resonance lines are clearly resolved [Figs. 1(a) and (b), Figs. 2(a) and (b)]. (II) Spectra in which the resonance lines have merged to the extent that they are no longer resolvable [Figs. 1(c) and 2(c)]. Further merging of the lines ultimately results in a Lorentzian-shaped spectrum [Figs. 1(d) and 2(d)]. (III) Spectra which appear to be "three-peaked," [Figs. 1(e) and 2(e)]. Class-I and -II spectra are symmetric with respect to the spectrum center. Class-III spectra are asymmetric. The class-I and -II spectra for all samples are interpreted in the present paper.

[48] Obtained from New England Nuclear Corporation.

[49] O. C. Kistner and A. W. Sunyar, Phys. Rev. **139**, B295 (1965).
[50] H. Fraunfelder, D. E. Nagle, R. D. Taylor, D. R. F. Cochran, and M. M. Visscher, Phys. Rev. **126**, 1065 (1961).
[51] W. A. Steyert and R. D. Taylor, Phys. Rev. **134**, A716 (1964).

The class-III spectra demonstrate a marked change in the character. These spectra apparently consist of a quadrupole split doublet superimposed on a single line. The relative intensity of the doublet increases with Fe concentration. The line separation of the doublet is insensitive to Fe concentration. These spectra will be interpreted in Paper II of this paper.

The source prepared from a pure (99.999%) gold foil (S-5) yielded a single resonance line at 2.4°K. Therefore, if the Au matrix can become polarized it must occur below this temperature.

The isomer shifts of the S-5 resonance line, the class-I spectra of the seven Au-Fe absorbers, and the central peak of the class-III spectra are all equal within ±0.02 mm/sec.

B. Methods of Analysis

The extraction of the hyperfine field at the nucleus, the quadrupole coupling, and the isomer shift from the class-I and class-II spectra are specified in the Appendix.

The effective absorber thickness for AuFe-7 at 77°K temperature is $t=2.2$ and remains nearly constant down to 4.8°K. All other samples have a smaller effective thickness. Therefore, in the magnetic hyperfine spectrum the effective absorber thickness per line is <0.4 for all samples. This is small enough so that line broadening due to absorber thickness and the interference effects due to overlapping absorption lines are both negligible.[52] The six lines of the magnetic hyperfine spectrum are labeled 1 through 6, where line 1 corresponds to the lowest energy.

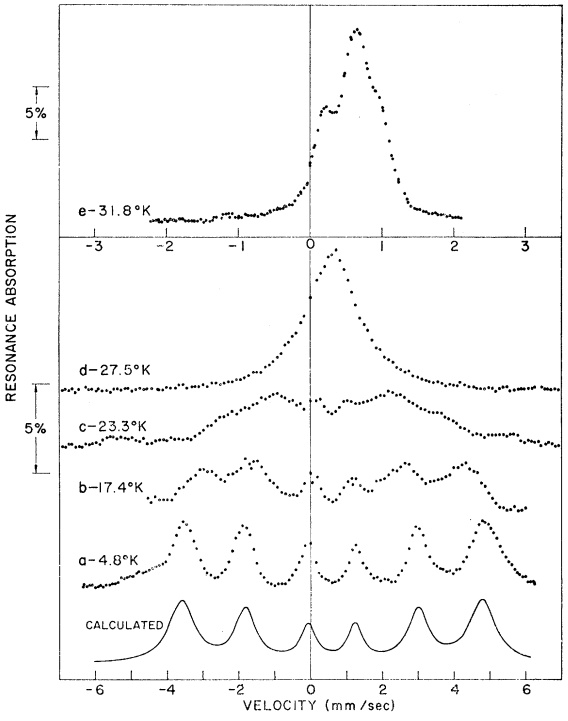

FIG. 1. Resonance absorption spectra of sample AuFe-7 (6.7 at.% Fe concentration) at various temperatures. The single line source (Co^{57} in Pd) was at room temperature. The calculated spectrum is obtained from Eq. (6) (for which the quadrupole coupling is zero) for a field width of 10%. The presence of a small positive quadrupole coupling is apparent in (a).

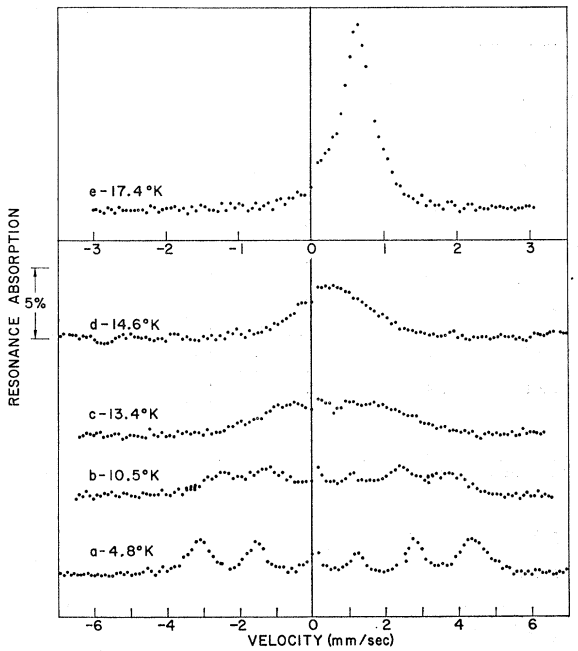

FIG. 2. Resonance absorption spectra of sample AuFe-9 (1.7 at.% Fe concentration) at various temperatures. The single line source (Co^{57} in Pd) was at room temperature.

VI. RESULTS

A. General Characteristics of the Class-I Spectra

The class-I magnetic hyperfine spectra exhibit the following characteristics:

(a) Each individual resonance line is symmetric.

(b) No resonance line has resolvable structure.

(c) The linewidths are symmetric with respect to the spectrum center and increase with distance from the center. Linewidths for AuFe-7 and AuFe-9 which have been designated Γ_3 (lines 1 and 6), Γ_2 (lines 2 and 5) and Γ_1 (lines 3 and 4) are given in Table I.

(d) Linewidths are relatively insensitive to the Fe concentration (see Table I).

(e) Line intensities as measured by the area under the absorption peak are in the ratios 3:2:1:1:2:3 to within ±10%.

(f) There is no detectable unsplit paramagnetic component superimposed on the magnetic hyperfine spectra.

[52] For a discussion of interference effect of overlapping resonance lines, see e.g., C. E. Violet and Rex Booth, University of California Radiation Laboratory Report No. UCRL-12438 1965 (unpublished).

TABLE II. Summary of results.

Sample	Iron concentration (at.%)																$T_0(x)$ (°K)	$g_0(0,x)$ (mm/sec)
Au S-5	$<10^{-4}$	T[a]	2.4														<2.4	<0.03
		g_0[b]	<0.03															
Au-Fe 2	0.84	T	2.4	4.8													11 ± 1	2.65 ± 0.08
		g_0	2.61	2.49														
Au-Fe 9	1.7	T	2.4	4.8	6.3	7.4	8.6	9.7	10.5	11.4	12.6	13.4	14.6				14.8 ± 0.5	2.82 ± 0.03
		g_0	2.78	2.75	2.67	2.60	2.43	2.39	2.28	2.20	2.02	1.62	0.70					
Au-Fe 3	1.9	T	2.4	4.8													16 ± 1	2.83 ± 0.08
		g_0	2.81	2.76														
Au-Fe 11	2.9	T	4.8	9.4	12.6												17 ± 1	2.88 ± 0.06
		g_0	2.82	2.60	2.30													
Au-Fe 8	4.4	T	4.8	10.0	13.6	14.6	15.5	16.6	20.9	21.5	23.3						23.5 ± 0.5	3.07 ± 0.03
		g_0	3.04	2.88	2.74	2.68	2.58	2.44	1.98	1.28	0.54							
Au-Fe 7	6.7	T	4.8	7.4	9.6	11.6	13.5	15.4	17.4	19.2	21.0	23.3	24.1	25.5	26.3	27.3	27.5	27.6 ± 0.5	3.12 ± 0.03
		g_0	3.09	3.07	2.97	2.94	2.87	2.79	2.68	2.46	2.30	1.95	1.78	1.56	1.14	0.875	0.486		
Au-Fe 1	7.4	T	2.4	4.8	21.0	27.9												27.8 ± 1.5	3.13 ± 0.06
		g_0	3.12	3.09	2.32	0.42													

[a] Temperatures are in °K. All values of g_0 were obtained with ascending temperature.
[b] g_0 is in units of 1 mm/sec which corresponds to 4.80×10^{-8} eV or 11.6 Mc/sec.

(g) The total resonance absorption in the class-I spectra equals that of the class-III spectra to within $\pm10\%$ for sample temperatures of 78°K or less.

(h) The ratio of the excited state splitting to the ground state splitting, g_1/g_0, is the same as in metallic Fe.

From (a), (b), and (c) one concludes that these spectra are not clearly resolvable admixtures of distinguishable Fe^{57} spectra and, the hyperfine field has a well-defined average value for all Fe atoms in the alloy. This is in marked contrast to the Mössbauer spectra of Cu-Fe alloys.[34,53]

The line broadening that occurs in the magnetically ordered state as described by (c) and (d) implies that the hyperfine field may be distributed with a small but observable characteristic width.

From (e) it follows that the hyperfine field taken over the bulk of the sample has a random orientation.[50]

Since the statistical accuracy of the experimental points is a few tenths of 1%, then it follows from (f) that below the ordering temperature less than 1% of the Fe atoms in the alloy have a hyperfine field of zero.

From (g) it is clear that essentially all of the Fe that exists in the paramagnetic state also exists in the magnetically ordered state. If a so-called "noise spectrum" exists as proposed by Klein,[14] it must contain less than 10% of the total Fe present. Since the ratio of g_1/g_0 in these alloys is the same as in metallic Fe relaxation effects are probably small.

B. Determination of $g_0(0,0)$ and T_0

By analogy with the law of corresponding states, we assume the relative magnetic ordering ($|H(T,x)|/|H(0,x)|$) scales with the reduced temperature $[T/T_0(x)]$, i.e.

$$\frac{|H(T,x)|}{|H(0,x)|}=F\left(\frac{T}{T_0(x)}\right), \tag{1}$$

where

$|H(T,x)|$ = magnitude of the hyperfine field at T°K,
$T_0(x)$ = transition temperature,
x = atomic fraction of Fe.

The relationship between $|H(T,x)|$ and the splitting of the ground state $g_0(T,x)$ and the first excited state $g_1(T,x)$ has been established experimentally,[54] i.e.,

$$\frac{|H(T,x)|}{g_0(T,x)}=(84.3\pm0.8)\frac{\text{kOe}}{\text{mm/sec}},$$

$$\frac{3g_1(T,x)}{g_0(T,x)}=1.715\pm0.004,$$

and our results can be expressed in terms of any one of these three quantities. We have arbitrarily chosen $g_0(T,x)$. Thus Eq. (1) can be written $g_0(T,x)/g_0(0,x)=F[T/T_0(x)]$.

The form of $F[T/T_0(x)]$ is unknown *a priori*. However, unique values of T_0 and $g_0(0,x)$ can be found for *each* sample such that Eq. (1) is satisfied for *all* samples within experimental error (2–7%). The resulting values of $g_0(0,x)$ and $T_0(x)$ are given in Table II. A plot of $g_0(T,x)/g_0(0,x)$ against $T/T_0(x)$ for all samples is shown in Fig. 3. The empirical curve obtained from Mössbauer resonance measurements on α-Fe^{54} and a "Brillouin curve" for a spin, $S=1$, are plotted in Fig. 3. The "Brillouin curve" is obtained by eliminating "y" from the equations

$$\frac{H(x,T)}{H(x,0)}=B(S,y), \quad \frac{H(x,T)}{H(x,0)}=y\frac{S+1}{3S}\frac{T}{T_c},$$

[53] W. Marshall, T. E. Cranshaw, C. E. Johnson, and M. S. Ridout, Rev. Mod. Phys. **36**, 399 (1964).

[54] R. S. Preston, S. S. Hanna, and J. Heberle, Phys. Rev. **128**, 2207 (1962).

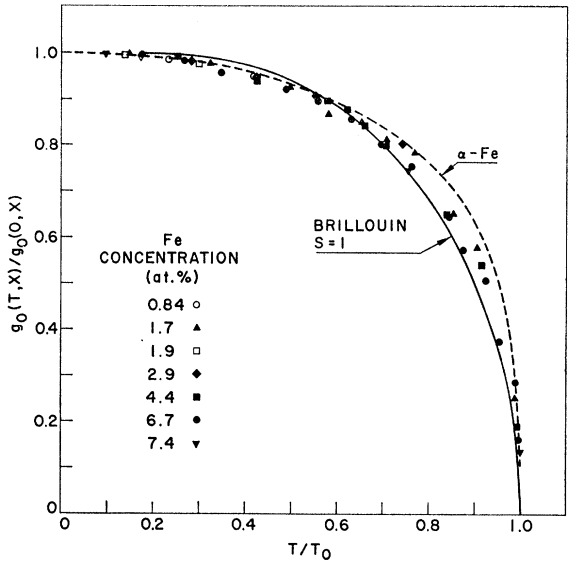

FIG. 3. The ground-state splitting $g_0(T,x)$ as a function of sample temperature T and Fe concentration x normalized to $g_0(0,x)$, the ground-state splitting at 0°K, plotted against the ratio of the sample temperature to the magnetic transition temperature. The rms error in $g_0(T,x)/g_0(0,x)$ is $\approx 2\%$ for $1.0 \lesssim T/T_0 \lesssim 0.9$ (class-I spectra) and $\approx 7\%$ for $0.9 \lesssim T/T_0 \lesssim 1.0$ (class-II spectra).

where $B(S,y)$ is the Brillouin function. These curves fit the points only qualitatively over the entire range of $T/T_0(x)$.

C. Dependence of $g_0(0,x)$ on Fe Concentration

The ratio of the ground-state splitting in the sample to that in α-Fe at 0°K, $[g_0(0,x)/g_0(0)_{\alpha-\mathrm{Fe}}]$, is plotted against Fe concentration in Fig. 4. We take as the ground-state splitting in α-Fe at 0°K, $g_0(0)_{\alpha-\mathrm{Fe}}=4.015 \pm 0.008$ mm/sec.[54] As shown in Fig. 4, the data of Gonser *et al.*[34] and Craig and Steyert[33] are in good agreement with our values.

According to Craig *et al.*[55] the hyperfine field as a function of x in Pd-Fe alloys is described by an equation

$$H(0)=H_{x=0}(0)P_0(x)+H_{x=1}(0)[1-P_0(x)], \quad (2)$$

where $P_0(x)$ is the probability that any Fe atom has no nearest neighbors, i.e., $P_0(x)=(1-x)^{12}$ in the fcc Pd (or Au) structure.

Equation (2) stems from the assumption that the hyperfine field is proportional to the conduction-electron polarization which in turn is the sum of the contribution from Fe with no nearest neighbors and from Fe with one or more nearest neighbors. To compare our results with the Pd-Fe system, we express Eq. (2) in the form

$$1-\frac{g_0(0,x)}{g_0(0)_{\alpha-\mathrm{Fe}}}=K(1-x)^z, \quad (3)$$

where

$$K=1-\frac{g_0(0,0)}{g_0(0)_{\alpha-\mathrm{Fe}}},$$

and $g_0(0,0)$ is the ground state splitting at 0°K in the limit of infinite dilution. The parameters K and z are determined by least-squares fitting. This results in

$$\frac{g_0(0,0)}{g_0(0)_{\alpha-\mathrm{Fe}}}=0.66\pm 0.03, \quad (4)$$
$$z=5.8\pm 0.9.$$

The ratio $g_0(0,x)/g_0(0)_{\alpha-\mathrm{Fe}}$, for these parameters is plotted in Fig. 4. Comparing these results with those of Craig *et al.*[55] it is clear that the Fe concentration dependence of the hyperfine field in Au-Fe alloys differs significantly from that in the Pd-Fe system.

According to Eq. (4) the value of the hyperfine field as the Fe concentration approaches zero is

$$\lim_{x\to 0}|H(0,x)|=223\pm 4 \text{ kOe}.$$

This can be compared to the saturation field obtained by Kitchens *et al.*[56] from very dilute Fe impurities in Au using an applied magnetic field

$$\mathbf{H}_{\mathrm{sat}}=-195\pm 2 \text{ kOe}.$$

The difference between these values may result from the following possibilities: (1) Eq. (3) may not be valid for $x<0.8$ at.%, which would make our extrapolated value incorrect; or (2) the applied field in the experiment in Kitchens *et al.*[56] may introduce significant contributions to the effective field at the nucleus which are absent in our experimental method.

It is curious to observe that our derived value of z is consistent with the number of next-nearest neighbors (6) in the fcc lattice, whereas the value assigned by Craig *et al.*[55] ($Z=12$) to explain the Pd-Fe data corresponds to the number of nearest neighbors (or next-next-nearest neighbors).

D. Characteristic Width of the Hyperfine Field

The broadened resonance lines of the magnetic hyperfine spectra is characteristic of the Au-Fe system. The observed broadening in Au-Fe might be caused by relaxation time effects[41,42] of a distributed hyperfine field with a characteristic width ΔH. An estimate of ΔH can be obtained by an examination of the effect of a field distribution on the hyperfine spectrum and comparing with the observed spectra.

To accomplish this we make the *ad hoc* assumption that the observed linewidth (Γ_0) is the sum of the source and absorber characteristic widths (Γ_N) and an incremental width (Γ^H) produced by ΔH, i.e.,

$$\Gamma_0=\Gamma_N+\Gamma^H. \quad (5)$$

[55] P. P. Craig, B. Mozer, and R. Segnan, Phys. Rev. Letters 14, 895 (1965).

[56] T. A. Kitchens, W. A. Steyert, and R. D. Taylor, Phys. Rev. 138, A467 (1965).

Line broadening due to absorber thickness can be neglected.

The incremental width in a resonance line, say line 1 or 6 ($\Gamma_3{}^H$), can be expressed in terms of the ground-state splitting as follows:

$$\Gamma_3{}^H=\gamma_0 g_0\beta_3,$$

where

$$\gamma_0=\frac{|\Delta H|}{|H(T,x)|}=\frac{\Delta g_0}{g_0(T,x)},$$

and

$$\beta_3=\tfrac{1}{2}\left(1+\frac{3g_1}{g_0}\right) \quad \text{(lines 1 and 6)}.$$

Thus, each line is broadened in proportion to its relative displacement, β, and the absolute value of the field width ΔH. This trend is substantiated by the results given in Table II. We can now write down an equation consisting of a sum of six Lorentzians which describes the total absorption spectrum in the presence of a distributed and randomly oriented hyperfine field

$$\begin{aligned}A\propto{}&3\Lambda_3[1+(\Lambda_3V_3^-)^2]^{-1}+2\Lambda_2[1+(\Lambda_2V_2^-)^2]^{-1}\\&+\Lambda_1[1+(\Lambda_1V_1^-)^2]^{-1}+\Lambda_1[1+(\Lambda_1V_1^+)^2]^{-1}\\&+2\Lambda_2[1+(\Lambda_2V_2^+)^2]^{-1}+3\Lambda_3[1+(\Lambda_3V_3^+)^2]^{-1},\end{aligned} \tag{6}$$

where

$A=$resonance absorption,

$$\Lambda_{1,2,3}=\left(1+\frac{\gamma_0}{2}g_0\beta_{1,2,3}\right)^{-1},$$

$$V^{\pm}{}_{1,2,3}=(\beta_{1,2,3}g_0\pm v),$$

$$\beta_2=\tfrac{1}{2}\left(1+\frac{g_1}{g_0}\right), \quad \text{(lines 2 and 5)};$$

$$\beta_1=\tfrac{1}{2}\left(1-\frac{g_1}{g_0}\right), \quad \text{(lines 3 and 4)};$$

$v=$source absorber relative velocity (positive for decreasing distance), $g_0=$ground state splitting in units of $\Gamma_N/2$.

This equation gives a good qualitative description of the class-I spectra for a field width of about 10% as shown in Fig. 1.

If relaxation effects are operative, the incremental linewidth would depend on the magnetic quantum numbers associated with the transitions.[57] Therefore, the observed linewidths would be compounded from a more complex relationship than Eq. (5). A more detailed and quantitative analysis would be required to determine the actual line-broadening mechanisms.

Other causes of line broadening which might conceivably be operative are (1) concentration fluctuation, (2) statistical fluctuations, and (3) instrumental broadening. These mechanisms, which are discussed in the following three paragraphs, have a negligible effect.

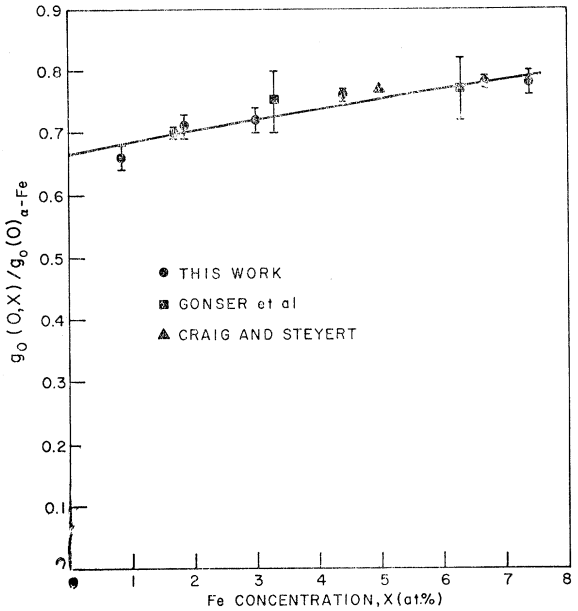

FIG. 4. The variation of the ground-state splitting at 0°K, $g_0(0,x)$, as a function of the Fe concentration x normalized to the 0°K ground-state splitting in α-Fe. Craig and Steyert do not quote an error.

(1) If the Fe in these Au-Fe samples existed in Fe-rich clusters as proposed by Crangle and Scott,[38] then fluctuations in the Fe concentration of such clusters could conceivably produce a distribution in the effective field. However, the hyperfine field is such a weak function of Fe concentration (see Fig. 4) that unreasonably large fluctuations in concentration would have to be postulated to account for the increased linewidths. For example, a spread in the hyperfine field of 10% would, according to Fig. 3, correspond to a spread in Fe concentration of a factor of 2 for $x=0.067$ (AuFe-7) and a factor of 10 for $x=0.017$ (AuFe-9).

(2) If unique values of the hyperfine field are associated with various configurations of nearest or next-nearest neighbors, then random fluctuation in these neighbors could cause an increase of linewidth. If this were the case the spread in the hyperfine field would increase with Fe concentration. Since the Fe in the Au-Fe samples of this experiment increases by approximately a factor of 10, the linewidths of AuFe-1 (7.4 at.%) Fe should be about a factor of three greater than those of AuFe-2(0.84 at.%). Since this readily observable effect is not present, random fluctuations in Fe neighbors appear to have no effect on linewidth.

(3) The velocity resolution of the spectrometer in the range $0\leq|v|\lesssim 10$ mm/sec is $|\Delta v/v|\approx 0.7\%$.[44] This is too small to account for the observed line broadening.

E. Dependence of $T_0(x)$ on Fe Concentration

The transition temperatures which were obtained by scaling $g_0(T,x)$ and T as described in Sec. B are plotted

[57] M. Blume (private communication).

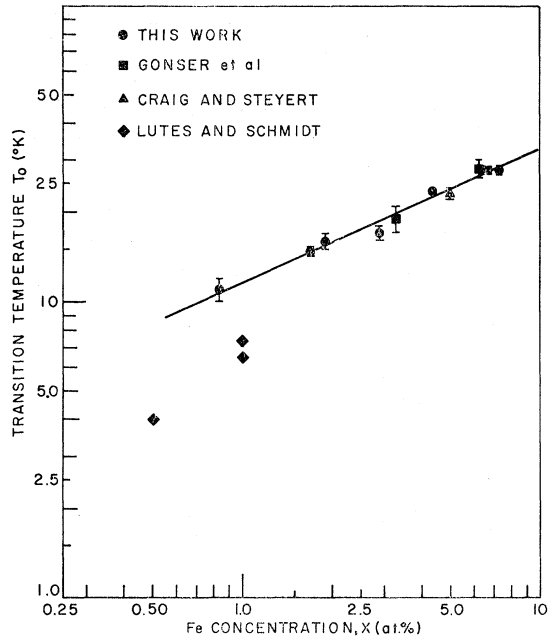

FIG. 5. The dependence of the magnetic transition temperature $T_0(x)$ on Fe concentration x.

against Fe concentration in Fig. 5. When an equation of the form

$$T_0(x)=Cx^n, \tag{7}$$

is fitted by least-squares to these results, we find

$$C=(11.6\pm0.3)\text{°K}/(\text{at.}\%)^n,$$
$$n=0.45\pm0.04.$$

The transition temperature is constrained by Eq. (7) to approach zero as $x\rightarrow 0$. This behavior of the transition temperature for concentrations less than 0.84 at.% Fe has yet to be demonstrated experimentally. Since our pure Au sample (S-5) exhibited no detectable splitting at 2.4°K, and upper limit on the transition temperature can be specified in the limit of infinite dilution, i.e.,

$$T_0(x\rightarrow 0)<2.4\text{°K}.$$[58]

Gonser *et al.*[34] combined their results with those of BBV and Lutes and Schmidt[31] and fitted Eq. (7) to the combined results for $x\lesssim 16$ at.% Fe concentration. The resultant value of the exponent was $n=0.74$. We have not combined the results of other experimenters with ours because (1) the transition temperatures obtained from the bulk magnetization measurements of Lutes and Schmidt appear to be significantly lower than the Mössbauer transition temperatures; (2) the method of Gonser *et al.*[34] and Craig and Steyert[33] of determining transition temperatures differs from our method; and (3) since a significant change in the Mössbauer spectrum occurs at 8–10 at.% Fe, it could be misleading to include results for Fe concentrations greater than 8 at.%, at least until the more concentrated region is better understood. Nevertheless, the transition temperatures reported by Gonser *et al.*[34] and Craig and Steyert[33] and the paramagnetic Curie temperature reported by Henry[30] are in good agreement with ours in the dilute region.

The relationship between the transition temperature as obtained by our method of analysis and transition temperatures obtained by other experimental methods has yet to be determined.

F. Quadrupole Coupling

The magnetic hyperfine spectra of all samples have been examined by the method specified in Sec. B of the Appendix for the possible presence of quadrupole coupling. Quadrupole coupling is detectable in the spectra of AuFe-7 and AuFe-1 from the characteristic shift of the hyperfine lines. It is not detectable, however, in the more dilute alloys. Measured values of this shift ϵ,[59] for AuFe-7 and AuFe-1, are plotted against T/T_0 in Fig. 6. The fact that ϵ is a positive quantity suggests that the hyperfine field direction and the electric field gradient symmetry axis are nearly collinear.

G. Isomer Shift

The isomer shift associated with the class-I spectra of all samples relative to the Pd source at room temperature is $\delta=+0.60\pm0.02$ mm/sec (see Sec. C of the Appendix). The isomer shift has no detectable dependence on Fe concentration. Our determination of the isomer shift of Fe in a Pd absorber relative to Fe in α-Fe source at room temperature is $+0.20\pm0.01$ mm/sec. Therefore, the isomer shift for these samples below their ordering temperature relative to α-Fe

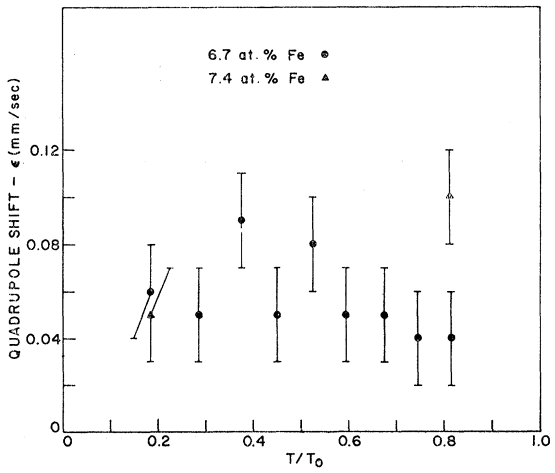

FIG. 6. The quadrupole shift ϵ, plotted against the ratio of sample temperature to magnetic transition temperature, T/T_0.

[58] According to the work of Kitchens *et al.* (Ref. 56), $T_0(x\rightarrow 0)<0.46$°K.

[59] O. C. Kistner and A. W. Sunyar, Phys. Rev. Letters 4, 412 (1960).

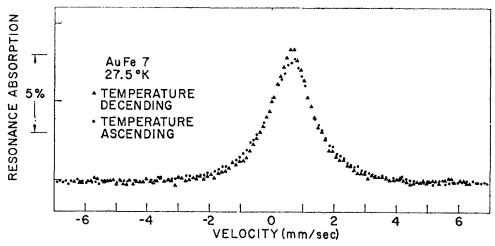

FIG. 7. Temperature hysteresis in AuFe-7 (6.7 at.% Fe concentration).

source at room temperature is $\delta = +0.80 \pm 0.02$ mm/sec. in agreement with the results of Kitchens *et al.*[56]

H. Temperature Hysteresis

All data given in Table I and plotted in Fig. 5 were taken with ascending sample temperature. To check on the possible presence of temperature hysteresis,[60] measurements of the apparent full width at half-maximum (Γ_0^A) of the total resonance spectrum for the class-II spectra of AuFe-7 and AuFe-9 were measured for ascending ($T\uparrow$) and descending ($T\downarrow$) sample temperatures. The results in terms of the ratios $\Gamma_0^A(T\uparrow)/\Gamma_0^A(T\downarrow)$ are given in Table III. The two spectra corresponding to the temperature of maximum effect for AuFe-7 are shown in Fig. 7. Temperature hysteresis is observed in AuFe-7, but not in AuFe-9. This effect is not detectable in AuFe-7 for temperatures less than 23.3°K. Temperature hysteresis has been searched for in the class-I spectra of AuFe-7 and AuFe-9, but no such effect is observable.

TABLE III. Temperature hysteresis.

Sample	Sample Temp. (°K)	$\Gamma_0^A(T\uparrow)/\Gamma_0^A(T\downarrow)$
AuFe-7	24.1	1.06±0.03
	25.5	1.08±0.03
	26.3	1.08±0.03
	27.3	1.12±0.03
	27.5	1.14±0.05
	29.6	1.05±0.09
AuFe-9	13.4	1.00±0.03
	14.6	0.92±0.05
	15.5	1.00±0.05
	16.7	1.00±0.10

VII. DISCUSSION

The nonlinear dependence of the transition temperature with Fe concentration, originally adumbrated by BBV, was confirmed by Gonser *et al.*[34] and by our results as well. In the region 0.8–8.0 at.% Fe concentration, the transition temperature varies essentially as the square root of the Fe concentration. This result is in clear disagreement with the generally presumed linear dependence which indeed is a consequence of the Curie-Weiss model.

Most of the recent theoretical work has been prompted by measurements of the magnetic properties of the Cu-Mn system, and subsequent justification of these theories has depended primarily upon the agreement with the Cu-Mn data. However, an examination of the literature reveals less than a half dozen measurements of T_0 in the concentration range appropriate to the theory. Furthermore, a linear relationship between T_0 and the Mn concentration is by no means apparent, and it would seem that much additional data are needed to define the proper relationship in Cu-Mn.

Klein[14] has recently proposed a model in which the magnetic interaction couples the solute atoms within small clusters by means of the Ruderman-Kittel-Yosida potential. The model is moderately successful in calculating the specific heat anomaly, but provides no method of directly calculating T_0 as a function of composition. It is also a consequence of this model that no well-defined transition temperature exists. Rather, the randomly oriented moments become increasingly correlated in an antiferromagnetic manner as the temperature decreases. However, the Mössbauer observations demonstrate that well-defined magnetic transition temperatures exist for Au-Fe alloys, contrary to Klein's theory.

The measured isomer shift indicates that the electron *charge* density at the Fe nucleus in these alloys is smaller than in metallic Fe. It also indicates that the electron charge density has no detectable variation with Fe concentration between 0.8–0.8 at.%. However, the measured dependence of the field at the Fe nucleus suggests that the electron *spin* density at the Fe nucleus varies with Fe concentration. Other (e.g. dipolar) contributions may also be contributing to the hyperfine field.

Based on present experimental data it can be concluded that an indirect exchange interaction is operative in dilute Au-Fe solid solutions. However, a model which explains the salient experiment facts has yet to be proposed.

ACKNOWLEDGMENTS

The assistance of Rex Booth, P. E. Bolduc, and D. N. Pipkorn in conducting these experiments has been invaluable. We are grateful to H. Patton and W. Brunner for the preparation of samples by vacuum evaporation and to W. Morris for the chemical analysis of the samples. During the conduct of these experiments we have had helpful discussions with C. Kittel, R. Watson, M. Blume, and T. A. Kitchens.

[60] L. F. Bates, *Modern Magnetism* (Cambridge University Press, New York, 1961), 4th ed.

APPENDIX: METHODS OF SPECTRA ANALYSIS

A. Determination of g_0

1. Class-I spectra

Let us specify the positions of the resolved resonance lines in order of increasing energy by x_n where $n=1, 2, \cdots, 6$. Now g_0 is obtained not from the line positions *per se*, but from their first differences $X_{nm}=x_n-x_m$. From six observations, a total of fifteen first differences can be generated. However, in combining measurements of a given quantity we are restricted to the combination of *independent* measurements only. Since there are only three independent first differences available from six observations, a given magnet hyperfine spectrum yields three independent measurements of g_0. These first differences can be chosen in several ways. There are, in fact, fifteen groups of three independent first differences available. These are specified in Table IV. The problem now is to determine which group (if any) provides the best determination of g_0.

We write the three prospective independent measurements of g_0 as follows:

$$\begin{aligned} g_{01}&=X_{nm}{}^{(1)}/f_1,\\ g_{02}&=X_{nm}{}^{(2)}/f_2,\\ g_{03}&=X_{nm}{}^{(3)}/f_3, \end{aligned} \tag{A1}$$

where the first difference $X_{nm}{}^{(1),(2),(3)}$ and the corresponding parameters $f_{1,2,3}$ for any group are specified in Table IV. The most probable value of g_0 is obtained by taking the weighted mean

$$g_0=\frac{w_1g_{01}+w_2g_{02}+w_3g_{03}}{w_1+w_2+w_3}, \tag{A2}$$

where $w_{1,2,3}$ are the weights.

Since the weight of a measurement is inversely proportional to the square of the absolute uncertainty, we have

$$\begin{aligned} w_1&\propto (f_1/\Delta X_{nm}{}^{(1)})^2,\\ w_2&\propto (f_2/\Delta X_{nm}{}^{(2)})^2,\\ w_3&\propto (f_3/\Delta X_{nm}{}^{(3)})^2, \end{aligned} \tag{A3}$$

where $\Delta X_{nm}{}^{(1),(2),(3)}$ are the uncertainties in the first differences.

The inherent statistical uncertainty in a line-position measurement is approximately proportional to $\Gamma_0/\sqrt{N}$ where N is the number of data points in the line. In these spectra $N\approx\Gamma_0$ approximately. Therefore, the expected statistical uncertainty varies roughly as $\sqrt{\Gamma_0}$. To obtain an estimate of the expected statistical uncertainties, we can take the linewidths of AuFe-7 from

TABLE IV. Values of f and $\mathfrak{F}$.

First difference	f	$\mathfrak{F}$	First difference	f	$\mathfrak{F}$	First difference	f	$\mathfrak{F}$	First difference	f	$\mathfrak{F}$	First difference	f	$\mathfrak{F}$
(2–1)	$\frac{r}{3}$[a]		(3–1)	$\frac{2r}{3}$		(4–1)	$1+\frac{r}{3}$		(5–1)	$1+\frac{2r}{3}$		(6–1)	$1+r$	
(3–4)	$1-\frac{r}{3}$	1.88	(4–2)	1	1.30	(3–2)	$\frac{r}{3}$	0.87	(3–2)	$\frac{r}{3}$	0.62	(3–2)	$\frac{r}{3}$	0.48
(6–5)	$\frac{r}{3}$		(6–5)	$\frac{r}{3}$		(6–5)	$\frac{r}{3}$		(6–4)	$\frac{2r}{3}$		(5–4)	$\frac{r}{3}$	
(2–1)	$\frac{r}{3}$		(3–1)	$\frac{2r}{3}$		(4–1)	$1+\frac{r}{3}$		(5–1)	$1+\frac{2r}{3}$		(6–1)	$1+r$	
(5–3)	1	1.30	(5–2)	$1+\frac{r}{3}$	0.76	(5–2)	$1+\frac{r}{3}$	0.64	(4–2)	1	0.59	(4–2)	1	0.51
(6–4)	$\frac{2r}{3}$		(6–4)	$\frac{2r}{3}$		(6–3)	$1+\frac{r}{3}$		(6–3)	$1+\frac{r}{3}$		(5–3)	1	
(2–1)	$\frac{r}{3}$		(3–1)	$\frac{2r}{3}$		(4–1)	$1+\frac{r}{3}$		(5–1)	$1+\frac{2r}{3}$		(6–1)	$1+r$	
(5–3)	$1+\frac{r}{3}$	0.87	(6–2)	$1+\frac{2r}{3}$	0.62	(6–2)	$1+\frac{2r}{3}$	0.59	(6–2)	$1+\frac{2r}{3}$	0.50	(2–5)	$1+\frac{r}{3}$	0.47
(6–4)	$\frac{r}{3}$		(5–4)	$\frac{r}{3}$		(5–3)	1		(4–3)	$1-\frac{r}{3}$		(4–3)	$1-\frac{r}{3}$	

[a] $r=3g_1/g_0=1.715$.

Table II which give the ratios in the order of lines 1 through 6

$$1.4:1.1:1:1:1.1:1.4. \quad \text{(A4)}$$

In addition to the statistical uncertainty we must also take into account the uncertainty inherent in the graphical method of determining line positions. This was estimated from the independent measurements of two observers on the same spectral lines. The difference in the measurements of the two observers on the same line can be written

$$D=X'-X''.$$

Assuming the inherent error of each observer is the same ($\Delta X'=\Delta X''$) the rms error in determining a line position graphically can be taken as

$$\Delta X'=2^{-1/2}\Delta D,$$

where ΔD is the root mean square of D. We found that $\Delta X'$ for various line positions did not correspond to $\sqrt{\Gamma_0}$. Instead, it was nearly independent of line position. Therefore, the error in the graphical method of determining line position is much more significant than the statistical error and the latter can be ignored. $\Delta X'$ when averaged over all line positions becomes $\Delta X'=0.04$ mm/sec. This is the best estimate of the rms error in a line position. Using this information and substituting Eqs. (A1) and (A3) into Eq. (A2) we have

$$g_0=\frac{X_{nm}^{(1)}f_1+X_{nm}^{(2)}f_2+X_{nm}^{(3)}f_3}{F}, \quad \text{(A5)}$$

where

$$F=f_1^2+f_2^2+f_3^2.$$

The rms error in g_0 on the basis of internal consistency[61] is

$$\Delta g_0=\Delta X'\mathfrak{F}, \quad \text{(A6)}$$

where $\mathfrak{F}=(f_1+f_2+f_3)/F$.

We now assert that the best value of g_0 is that for which the associated uncertainty in g_0 is a minimum. Based on the above definition this occurs when $\mathfrak{F}$ is a minimum. We have arbitrarily chosen the group

$$X_{nm}^{(1)}=x_6-x_1,$$
$$X_{nm}^{(2)}=x_5-x_3,$$
$$X_{nm}^{(3)}=x_4-x_2,$$

for which $\mathfrak{F}$ has nearly its minimum value as the basis of the analysis. The corresponding rms error in g_0 is

$$g_0=0.03 \text{ mm/sec}.$$

2. Class-II spectra

For symmetric spectra where the resonance lines are not resolved, the hyperfine field can be obtained from the apparent full width at half "maximum," Γ_0^A. The "maximum" in this case is taken as the average height of the two highest peaks of the spectrum.

Values of Γ_0^A can be obtained graphically from plots of Eq. (6) with g_0 (expressed in units of $\Gamma_N/2$) and γ_0 as parameters. The resulting values can be expressed as

$$\frac{\Gamma_0^A}{\Gamma_N}-1=G(g_0).$$

The function $G(g_0)$ for $0\leq g_0\leq 3$ and $\gamma_0\approx 0$ is given to better than 5% by the polynomial

$$G(g_0)=0.26g_0+1.34g_0^2-0.56g_0^3+0.08g_0^4. \quad \text{(A7)}$$

This equation agrees with that of Kimball *et al.*[62] for $g_0>2$. However, for smaller values of g_0 the above equation predicts significantly smaller values of $[(\Gamma_0^A/\Gamma_N)-1]$ than does the equation of Kimball.

Values of g_0 as obtained from the measured values of Γ_0^A and Eq. (A7) are included in Table II.

There are a few spectra for each sample where the two methods of extracting g_0 can be compared. In no case did the two methods differ by more than 15%. The rms error in g_0 resulting from the use of Eq. (A7) can be estimated by assuming this deviation to be the 95% level of confidence. Therefore, the rms error in g_0 extracted from the class-II spectra is estimated as $\Delta g_0\approx 0.07g_0$.

B. Determination of the Quadrupole Coupling

The quadrupole coupling associated with these data is clearly small, relative to the magnetic interaction. Therefore, the shifts produced in the resonance lines of the class-I spectra are of equal *magnitude*.[58] The quadrupole shift, $\epsilon=\frac{1}{4}(e^2qQ)$ (using the conventional symbols), can be determined from the appropriate *second* differences obtained from the six line positions. The appropriate second differences are obtained from the *first* differences which involve lines 1 and 6, excluding the first difference (x_6-x_1). There are eight such first differences, namely

$$x_2-x_1=g_0\left(\frac{r}{3}\right)-2\epsilon, \qquad x_6-x_2=g_0\left(1+\frac{2r}{3}\right)+2\epsilon,$$

$$x_3-x_1=g_0\left(\frac{2r}{3}\right)-2\epsilon, \qquad x_6-x_3=g_0\left(1+\frac{r}{3}\right)+2\epsilon,$$

$$x_4-x_1=g_0\left(1+\frac{r}{3}\right)-2\epsilon, \qquad x_6-x_4=g_0\left(\frac{2r}{3}\right)+2\epsilon,$$

$$x_5-x_1=g_0\left(1+\frac{2r}{3}\right)-2\epsilon, \qquad x_6-x_5=g_0\left(\frac{r}{3}\right)+2\epsilon.$$

[61] R. T. Birge, Phys. Rev. **40**, 207 (1932).

[62] C. Kimball, W. D. Gerber, and A. Arrott, J. Appl. Phys. **34**, 1046 (1963).

The signs reflect the fact that ϵ is intrinsically positive for AuFe-7 and AuFe-1. The best values of ϵ are obtained by generating second differences such that g_0 and hence the error in g_0 vanishes, namely

$$\begin{aligned} Y^{(1)} &= (x_6-x_2)-(x_6-x_1), \\ Y^{(2)} &= (x_6-x_3)-(x_4-x_1), \\ Y^{(3)} &= (x_6-x_4)-(x_3-x_1), \\ Y^{(4)} &= (x_6-x_5)-(x_2-x_1). \end{aligned} \tag{A8}$$

All of the above second differences equal 4ϵ. Since these quantities are not independent of each other they must not be combined. Recalling that $\Delta X_{nm}{}^{(1),(2),(3)} \approx \Delta X'$ (=0.04 mm/sec) is independent of line position, one concludes that the best value of ϵ is obtained from any one of the four second differences above. We have arbitrarily chosen $Y^{(4)}$.

Since $\Delta X'$ is independent of line position, the error in a second difference is twice the error in the line position,

$$\Delta Y^{(4)} = 2\Delta X'.$$

The quadrupole shift is

$$\epsilon = \frac{Y^{(4)}}{4};$$

therefore the rms error in ϵ is

$$\Delta\epsilon = \frac{\Delta Y^{(4)}}{4} = \tfrac{1}{2}\Delta X = 0.02 \text{ mm/sec}.$$

We make no attempt to extract the quadrupole shift from the class-II spectra.

C. Determination of the Isomer Shift

For class-I spectra, the isomer shift is given by

$$\delta = \tfrac{1}{6}\left(\sum_{n=1}^{6} x_n - 2\epsilon\right). \tag{A9}$$

Substituting for ϵ any of the four second differences of Eq. (A8), one obtains for the rms error in the isomer shift

$$\Delta\delta = (\sqrt{7})/6\Delta X' = 0.02 \text{ mm/sec}.$$

If the quadrupole shift is *a priori* zero, the rms error from Eq. (A9) is

$$\delta = \Delta X'/\sqrt{6}.$$

The isomer shift of the class-II spectra can be estimated from the mid point of the $\Gamma_0{}^A$ measurement. Accordingly we have found no measurable difference in the isomer shift of the class-II compared to the class-I spectra.

PHYSICAL REVIEW VOLUME 149, NUMBER 2 16 SEPTEMBER 1966

High-Temperature Magnetic Susceptibility of Lanthanum and Cerium Metals*

C. R. Burr and S. Ehara
Department of Physics, University of California, Los Angeles, California
(Received 7 April 1966)

The magnetic susceptibilities of cerium and lanthanum metals have been measured from room temperature through the melting point. Cerium has a unique fusion behavior with a negative melting slope which has been attributed to a $4f$–$5d$ electronic promotion. It is demonstrated that this promotion in cerium does not occur and that the small change in the susceptibility at cerium's two high-temperature phase transformations can be attributed almost entirely to changes in the Pauli susceptibility. A quantitative estimate of this change is found by comparison with the lanthanum high-temperature susceptibility.

I. INTRODUCTION

DURING the past few years, careful attention has been paid to the magnetic properties of metallic cerium. The motivation for the present high-temperature susceptibility measurements comes from very recent work on the fusion curve of cerium by Jayaraman[1] in which he suggests that an electronic promotion of the $4f$ electron to the $5d$ conduction band occurs at the melting point for pressures below 30 kbar. The cerium fusion curve is unique in that it has an initially negative slope followed by a broad minimum. The phase diagram for cerium (Fig. 1) shows that as the pressure is increased below 275°C cerium undergoes an abrupt transformation from a γ phase to an α phase. Both phases possess face-centered-cubic (fcc) structure, but the lattice constant of the α phase is smaller than that of the γ phase. The γ-to-α transition is believed to end in a critical point.[2,3] If one extrapolates the transition line beyond the critical point, it meets the fusion curve at its minimum. At temperatures above the

* Supported in part by the National Science Foundation and the Office of Naval Research, Nonr 233 (88).
[1] A. Jayaraman, Phys. Rev. **137**, A179 (1965).
[2] R. I. Beecraft and C. A. Swenson, J. Phys. Chem. Solids **15**, 234 (1960).
[3] B. L. Davis and L. H. Adams, J. Phys. Chem. Solids **25**, 379 (1964).